J. Astrophys. Astr. (June 2017) 38:20
DOI 10.1007/s12036-017-9440-2

Spectroscopic Variability of Supergiant Star HD14134, B3Ia

Y. M. MAHARRAMOV

Shamakhy Astrophysical Observatory, Azerbaijan National Academy of Sciences, Yu. Mammadaliyev Settlement, Shamakhy District, Republic of Azerbaijan.
Corresponding author. E-mail: y_meherremov@rambler.ru

MS received 16 August 2016; accepted 20 March 2017; published online 19 June 2017

Abstract. Profile variations in the Hα and Hβ lines in the spectra of the star HD14134 are investigated using observations carried out in 2013–2014 and 2016 with the 2-m telescope at the Shamakhy Astrophysical Observatory. The absorption and emission components of the Hα line are found to disappear on some observational days, and two of the spectrograms exhibit inverse P-Cyg profile of Hα. It was revealed that when the Hα line disappeared or an inversion of the P-Cyg-type profile is observed in the spectra, the Hβ line is displaced to the longer wavelengths, but no synchronous variabilities were observed in other spectral lines (CII λ 6578.05 Å, λ 6582.88 Å and HeI λ 5875.72 Å) formed in deeper layers of the stellar atmosphere. In addition, the profiles of the Hα and Hβ lines have been analysed, as well as their relations with possible expansion, contraction and mixed conditions of the atmosphere of HD14134. We suggest that the observational evidence for the non-stationary atmosphere of HD14134 can be associated in part with the non-spherical stellar wind.

Keywords. HD14134 supergiant—spectroscopy—line profile variability.

1. Introduction

Studies of such hot supergiants, which are the brightest stars, is of enormous interest to our understanding of the stellar and chemical evolution of the Galaxy. The presence of emission lines in the optical spectra of hot supergiants has been known for decades. Their general interpretation regarding emission in an 'expanding shell' has been accepted for nearly as long (e.g., Swings & Struve 1940). It had been suspected on the basis of the line profiles, particularly Hα, that the stellar atmospheres were geometrically extended and probably expanding. Confirmation of mass loss via a stellar wind came with the observation of ultraviolet absorption lines with velocity shifts greater than the escape velocity (Morton 1967).

Previous surveys have been very useful in documenting Hα line-profile variability in OB stars (e.g. Ebbets 1982), but frequently suffered from a poor temporal sampling hampering the study of the line-profile variations on a rotational time-scale.

Among the most interesting characteristics of early B supergiants are the various kinds of spectroscopic variations. Due to the variable stellar wind, variations of the intensity, radial velocities, and P-Cygni profiles of lines of hydrogen, helium, and high-ionization ions are observed in the spectra of hot supergiants. High mass-loss rates are typical for the brightest stars. For example, the hot supergiant HD14134 studied in the present paper has a mass-loss rate of $\dot{M}$=1.45 $\times 10^{-6} M_{\odot}$/yr (Morel *et al.* 2004). The Hα line is an especially sensitive tracer of the mass-lose rate.

The supergiant star HD14134 belongs to the star with P Cyg profile of the Hα line. This star is a hot supergiant of spectral type B3Ia with the following parameters (Barlow & Cohen 1977; Kraus & Fernandes 2009; Vardya 1984; Morel *et al.* 2004; Crowther *et al.* 2006): $m_v = 6.55$ mag, $M/M_{\odot} = 24$, $R/R_{\odot} = 52$, $\log L/L_{\odot} = 5.24$, $T_{\rm eff} = 16300$ K, $\log g = 2.05$, $v \sin i = 66\,{\rm km\,s^{-1}}$, $d = 2.12$ kpc.

It is believed that this star belongs to Per OB1 association (Lennon *et al.* 1993).

Kudritzki *et al.* (1999) presented the results of the stellar wind analysis (the β exponent of the velocity low, v_{∞}, the terminal velocity and M, the mass loss rate) for several supergiants, including HD14134. They used the new unified model code developed by Santolaya-Rey *et al.* (1997). The Balmer lines of supergiants are analysed by means of NLTE (non-local thermodynamic equilibrium) unified model atmospheres to determine

the properties of their stellar winds, in particular, their wind momenta.

Morel *et al.* (2004) presented the results of a long-term monitoring campaign of the Hα line in a sample of bright OB supergiants which aims at detecting rotationally modulated changes potentially related to the existence of large-scale wind structure. It is noted that conspicuous evidence for variability in Hα is found for the stars displaying a feature contaminated by wind emission. Most changes took place on a daily time-scale. This survey has revealed the existence of cyclical Hα line-profile variations in HD14134. Also, photometric studies of this star found 12.8 days periodicity.

According to Prinja *et al.* (1996), the Hα line is at $r \sim 1.5R_*$ in O-type supergiants. Although the line-formation regions are likely to be more extended in B-type supergiants, this transition still probes the few inner radii of the stellar wind (Morel *et al.* 2004).

In the B-type supergiants a variety of complex profiles were observed. Researchers noted that the profile of Hα line in the spectra of HD14134 indicates fast variable structure, but the sequence of observations was irregular and inadequate to trace in detail the changes in the spectra. Therefore they noted that more systematic observations are needed to investigate this supergiant.

In the present paper, which is a sort of continuation of the above studies, we analysed variations of the Hα and Hβ lines.

We also investigated the variabilities of the CII (λ6578.05 Å, λ6582.88 Å) and HeI λ5875.72 Å lines which formed deeper effective layers in the atmosphere of those stars. Our main aim is to study the observed peculiarities of these lines in the spectra. Therefore we present the results of HD14134 (B3Ia), as well as their possible generalized interpretations.

We believe our results will be of interest for further studies of these remarkable stars.

2. Observations and data reduction

Spectral observations of HD14134 were carried out during 2013–2014 and 2016 using a CCD detector in the echelle spectrometer mounted at the Cassegrain focus of the 2-m telescope of the Shamakhy Astrophysical Observatory (Mikailov *et al.* 2005). The spectral resolution was R = 15000 and the spectral range is $\lambda\lambda$ 4700−6700 Å.

One to two spectra of the target stars were obtained on each night (Table 1). The signal-to-noise ratio was S/N =150–200. The average exposure was 1200–1500 s, depending on the weather conditions.

Table 1. The log of observations employed in this study.

Date	JD 2,450,000.00+	UT (h, min)	Exposure (s)
2013 Dec. 25	6652.33	19.51	1200
Dec. 29	6656.33	20.00	1000
Dec. 30	6657.31	19.30	900
2014 Feb. 07	6696.19	16.31	1500
Feb. 07	6696.21	17.04	1500
Feb. 09	6698.19	16.29	1800
Feb. 10	6699.18	16.20	1500
Feb. 10	6699.20	16.50	1500
Feb. 13	6702.17	16.11	1200
Feb. 13	6702.19	16.32	1200
Feb. 18	6707.19	16.34	1500
Feb. 18	6707.21	17.01	1500
Aug. 27	6897.37	20.46	1000
Aug. 27	6897.38	21.05	1000
2016 Feb. 13	7432.31	19.23	1800
Feb. 13	7432.33	19.55	1800
Feb. 15	7434.34	20.16	1800
Feb. 15	7434.37	20.48	1800

Our echelle spectra were performed using the MIDAS echelle package and Dech20 program package (Galazutdinov 1992), and all data were reduced.

The main steps of the reduction of the CCD images scheme were: correction of the dark noise; removal of cosmic rays; background subtraction; flat-field correction; extraction of one-dimensional spectra; wavelength calibration; correction for atmospheric H_2O vapour lines; normalization to continuum intensity; conversion to heliocentric velocity scale (measurements of radial velocities and equivalent widths for various spectral features).

We removed cosmic-ray traces via a median averaging two consecutive exposures.

As found in the cross-cut image of the object frame, the counts of the region between the two adjacent orders are not zero due to the background including scattered light inside the spectrograph. These should be subtracted as the background of the data. Estimates of background are made by masking the apertures of the spectra and applying surface fitting to the other regions.

The flat-field of the detector was determined using flood-light provided by a quartz lamp. Flat-field correction (i.e. correction for pixel-to-pixel intensity transfer function variability) has been done by smoothing a flat-field spectrum and normalizing the original flat-field

with the smoothed one. This normalized flat-field then was divided into the measurements.

The extraction of one-dimensional spectra from the flat-field and background-subtracted object frame is made.

We recorded the spectrum of a thorium–argon lamp for wavelength calibration. The stability of the wavelength scale was verified by measuring the wavelength centroids of OI and H_2O sky lines. The long term accuracy achieved for the wavelength calibration is of the order of $1\,\mathrm{km\,s^{-1}}$ as derived from the spread of measured radial velocities of telluric lines in the spectra.

Note that the atmospheric H_2O vapour absorption lines can affect the fine structure of line profiles since it may be difficult to distinguish them from weak intrinsic inflections or reversals. Therefore we recorded the spectrum of the rapidly rotating star HR1122 (B5III) each night, which has no narrow lines, for use in subtracting the telluric absorption spectrum. The water vapour lines in the pseudo-continuum regions around Hα were interactively shifted and scaled with the Dech20 task telluric until the residuals between the observed spectra and the template telluric spectrum were minimized.

Finally, the resulting wavelength-calibrated and flat-field spectra are merged, rebinned to heliocentric velocities and normalized by a spline fit to the continuum through predefined continuum windows.

The radial velocities for individual lines are measured by shifting the direct and mirrored images of their profiles horizontally to achieve the best matching.

The measurement error for the equivalent widths (W) does not exceed 5%, and error of the radial velocity (V_r) is of the order of $\pm 2\,\mathrm{km\,s^{-1}}$. Here, ($V_r$) are velocities of the absorption minima or emission maxima in the selected lines.

3. Results

During our observations, a large variety of Hα profile shapes of HD14134 were seen: complete absence and inverse P-Cygni profile.

There were two occasions at which the Hα line completely disappeared from the spectra. This behaviour is real and recurrent.

When the Hα line disappears or becomes faint, the Hβ line is displaced to the relatively longer wavelengths.

We also observed an inversion of the P-Cyg-type profile of the Hα line, and it is accompanied by a large redshift of the Hβ line profiles.

When the Hα line disappeared or an inversion of the P-Cyg-type profile is observed in the spectra, no significant variabilities were observed in other spectral lines (except Hβ) formed in deeper layers of the stellar atmosphere.

3.1 *Data analysis*

Observations show that the most pronounced variability in the spectra of HD14134 is noticeable in the intensity and profiles of the Hα line. The following shapes of the Hα profile were observed:

(a) Normal P-Cygni profile, (b) inverse P-Cygni profile, (c) pure absorption profile, (d) pure emission profile, (e) the emission profiles on both sides of central absorption component, and (f) complete absence.

Figure 1 shows the spectra of HD14134 in the wavelength ranges covering the Hα and Hβ regions observed in 2013–2014 and 2016. In Fig. 1, the spectra obtained on 25/12/2013, 29/12/2013, 30/12/2013 and 09/12/2014 are shown as individual profiles, but the rest of them are averaged as two expositions taken during single nights (see Table 1).

The profile of the Hα line observed in the atmosphere of the HD14134 supergiant indicates a rapidly variable structure.

On December 25, 2013 and on August 27, 2014, the Hα profile in the spectrum of the star HD14134 had the shape of an inverse P-Cygni profile (Fig. 1a). Another variability pattern occurred, where Hα appeared only in weak emission (13/02/2016).

The Hα line was absent in the spectra of December 29–30, 2013 and of February 15, 2016, while two carbon lines CII (λ6578.05 Å, λ6582.88 Å), as well as several weak stellar and atmospheric lines in the spectral order where Hα is located, in the region $\lambda\lambda 6400-6600$ Å were found (Figures 1 and 2). In these same spectra, all the other lines typical for hot supergiants such as HD14134, apart from Hα, are observed, including Hβ.

To investigate the short-term variability in the Hα profile, all individual spectra obtained on December 29–30, 2013, and on February 13, 15, 2016 were processed separately. These data are presented in Fig. 2. As can be seen, the Hα profile can be a variable on time scale of hours.

Unfortunately, weather conditions before and after December 29–30, 2013 and February 15, 2016, did not make it possible to obtain spectra of the star HD14134, which could shed light on the transition moments of this interesting process.

Our measurements show that the radial velocities and spectral parameters (W, the equivalent width, R, the

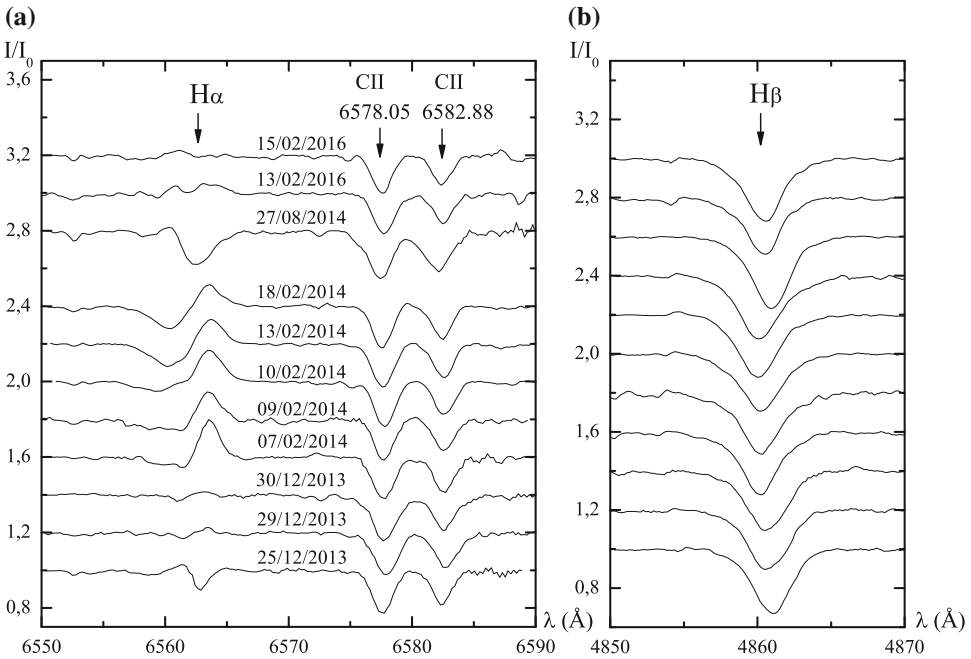

Figure 1(a), (b). Profiles of the Hα, CII (λ6578.05 Å, λ6582.88 Å), and Hβ lines in the spectra of HD14134 observed in 2013, 2014 and 2016.

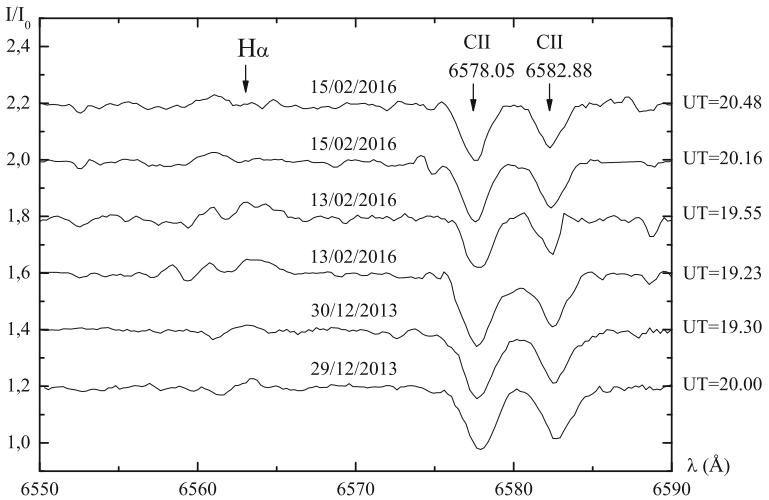

Figure 2. Hα and CII (λ6578.05 Å, λ6582.88 Å) profiles in the individual spectra of HD14134 observed in 2013 and 2016.

depth, r, the residual intensity and FWHM, the half-width) of the absorption and emission components of the Hα line, as well as the parameters of lines of other elements, vary with time.

Figure 1(a) shows that the absorption components of Hα are broader and shallow with very weak components in the spectra on February 07, 09–10, 2014. It is also interesting that formation of components in the absorption profiles of the Hα line decreases the depth and equivalent width of the line (see Table 2).

We measured the spectral parameters and radial velocities of Hα line. As seen from Table 2, significant changes occurred in the radial velocity and spectral parameters of these lines. Fig. 1(a) and Table 2 show that sometimes, Hα line absorption component is shifted toward the red side with a velocity of $-13\,\mathrm{km\,s^{-1}}$. Table 2 also shows that the radial velocity of the 'blue' component of the absorption line Hα varies from -179 to $-13\,\mathrm{km\,s^{-1}}$. The radial velocity of the Hα line emission component varies within the range of -128–17 $\mathrm{kms^{-1}}$. We have determined that the equivalent width, half-width and depth (in emission the residual intensities) of the absorption component of the Hα line vary within 0.14−0.56 Å, 1.3−4.2 Å, and

Table 2. Measurement of the parameters of the Hα line.

Date	JD	Hα							
	2,450,000.00+	V_r abs (km s^{-1})	V_r em (km s^{-1})	W abs (Å)	W em (Å)	R abs	r em	FWHM abs (Å)	FWHM em (Å)
2013 Dec. 25	6652.33	−13	−87	0.14	0.03	0.10	1.02	1.3	1.0
Dec. 29	6656.33	–	–	–	–	–	1.00	–	–
Dec. 30	6657.31	–	–	–	–	–	1.00	–	–
		−91							
2014 Feb. 07	6696.21	−88	11	0.14	0.35	0.05	1.20	3.4	1.7
		−210							
Feb. 09	6698.19	−95	7	0.24	0.28	0.06	1.14	4.2	1.9
Feb. 10	6699.20	−179	10	0.15	0.39	0.05	1.17	3.3	2.2
Feb. 13	6702.19	−142	17	0.36	0.28	0.12	1.13	3.1	2.1
Feb. 18	6707.21	−134	13	0.35	0.23	0.12	1.11	2.7	1.8
Aug. 27	6897.38	−31	−128	0.56	0.02	0.19	1.02	2.7	0.9
2016 Feb. 13	7432.33	–	–	–	–	–	–	–	–
Feb. 15	7434.37	–	–	–	–	–	1.00	–	–

Here V_r, W and FWHM are radial velocities, equivalent widths and half widths of the absorption and emission components of the line, respectively. R is the depth of the absorption and r is the residual intensity of the emission component of the line.

0.05−0.19 Å, the emission component varies within 0.02−0.39 Å, 0.9−2.2 Å, and 1.00–1.20 Å, respectively.

To investigate the reason for the variability of the Hα profile, the Hβ, lines of CII and HeI, and others were analysed in the spectra.

Table 3 shows that radial velocity, equivalent width, half-width and depth of the Hβ line varies from −97 to −30 km s^{-1}, 0.96−1.27 Å, 2.7−3.4 Å and 0.29−0.37 Å, respectively. As can be seen in Fig. 1 and Tables 2 and 3, when the inverse profile of Hα or the disappearance of this line is observed, the Hβ line is shifted towards the red simultaneously. The Hβ line profile also shows relatively structural changes (Fig. 1(b)).

Figure 1a shows that the shape of the CII lines changes relatively during observations, as well as the radial velocities of these lines varied between from −46 to −25 km s^{-1} (Table 3). Variability of the absorption lines indicates that disturbances are occurring fairly deep in the atmosphere of the star.

The investigation of the HeI λ5875.72 Å line showed that the radial velocity of this line varies from −53 to −35 km s^{-1} (Table 3), but its profile did not change substantially (Fig. 3).

According to Klochkova & Chentsov (2004), at any rate Hα, Hβ and the strongest absorption lines, as well as HeI line in the visual spectrum CygOB2-No.12 are partially formed in the wind. But the line-forming region for HeI might be substantially larger and may be extending into the base of the wind (Kraus *et al.* 2015).

Our measure of this line shows strong radial velocity variability and due to the significant line strength it is difficult to detect structural changes in the line profile. Still, the line profile is expected to be slightly variable.

The CII and HeI lines are formed in different regions in the atmosphere with CII originating in deeper layers (Kraus *et al.* 2015). Interestingly, the structures of the CII lines show relative variations, while the HeI λ5875.72 Å line remains almost constant.

It is known that the formation of neutral Na is not expected in the photosphere of such a hot star because of its very small ionization energy (Stahl & Wolf 1986). However, we observe NaID lines in the spectrum of the hot supergiant.

The region around the NaID lines is also shown in Fig. 3. The radial velocities of the NaI lines varied from −24 to −16 km s^{-1} respectively. The profiles of this line are seen with a single peak in our sample because of low resolution.

Klochkova *et al.* (2014) noted that two main components in the deepest part of the absorption of NaID are observed. That is, these components are observed separately with a higher resolution. They also noted that the red components of NaID line are of interstellar origin and form in the local arm of the Galaxy. The blue components of NaID form in the expanding circumstellar envelope of the star.

According to Stahl & Wolf (1986), the presence of NaID line in the spectrum of hot stars indicates

Table 3. Measurements of the parameters of the CII, HeI and Hβ lines.

Date	JD	CII 6578.05 Å	CII 6582.88 Å	HeI 5875.72 Å	Hβ			
	2,450,000.00.00+	V_r abs (km s^{-1})	V_r abs (km s^{-1})	V_r abs (km s^{-1})	V_r abs (km s^{-1})	W abs (Å)	R abs	FWHM abs (Å)
2013 Dec. 25	6652.33	−31	−37	−43	−30	1.11	0.33	3.0
Dec. 29	6656.33	−25	−30	−35	−71	1.09	0.30	3.4
Dec. 30	6657.31	−32	−30	−44	−74	1.10	0.30	3.3
2014 Feb. 07	6696.21	−34	−33	−44	−89	1.14	0.32	2.9
Feb. 09	6698.19	−36	−37	−48	−88	1.19	0.31	3.0
Feb. 10	6699.20	−32	−37	−41	−90	1.11	0.29	3.3
Feb. 13	6702.19	−39	−35	−53	−97	1.16	0.32	3.2
Feb. 18	6707.21	−42	−39	−53	−97	1.26	0.32	3.3
Aug. 27	6897.38	−42	−46	−38	−40	1.27	0.37	3.0
2016 Feb.13	7432.33	−34	−35	−43	−72	0.96	0.29	2.7
Feb. 15	7434.37	−38	−43	−46	−68	1.12	0.32	2.9

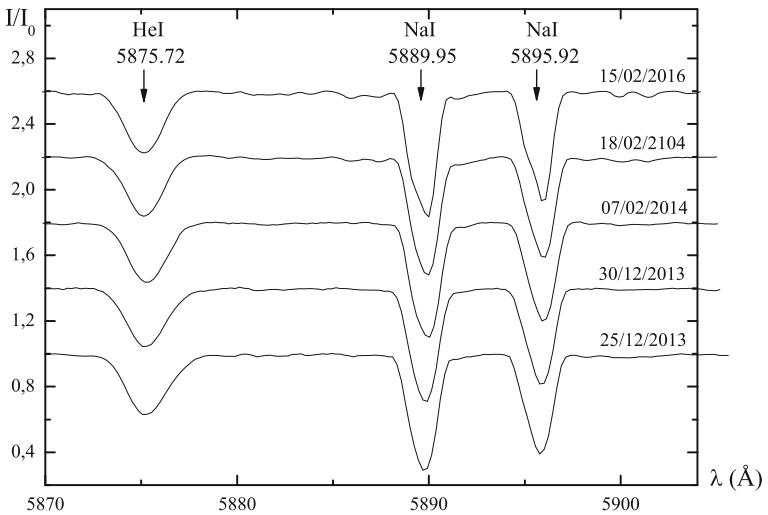

Figure 3. Profiles of the HeI λ5875.72 Å and NaI (λ5889.95 Å, λ5895.92 Å) lines in the spectra of HD14134 observed in 2013, 2014 and 2016.

that a sizeable fraction of the circumstellar matter is neutral.

So, NaID lines probably form at large distances from the central star. We suggest that these components form in the interstellar medium and/or in the circumstellar matter.

Also, some of the results of measurements in the spectra of HD14134 are presented on a time scale in Figures 4 and 5. It has been revealed that the variability of radial velocity, equivalent widths, depths and half-widths of Hβ line, as well as HeI λ 5875.72 Å and averaged CII (λ6578.05 Å, λ6582.88 Å) lines indicate repeating features.

The changes of the radial velocities and spectral parameters of line Hβ have been revealed (Fig. 4). The radial velocity of the line Hβ have been changed by 67 km s^{-1} (from −30 to −97 km s^{-1}) during ∼50−55 days. If this can be considered as an amplitude of variations, then the value of a variability period of a star can be considered in ∼100−110 days. Similar changes of HeI and CII lines with the low amplitude (∼18 km s^{-1} and ∼13 km s^{-1} respectively) during the same time have been observed (Fig. 4). These variabilities can be explained by the pulsation. For a more precise determination of pulsation period of star, the systematic observations of this star are necessary.

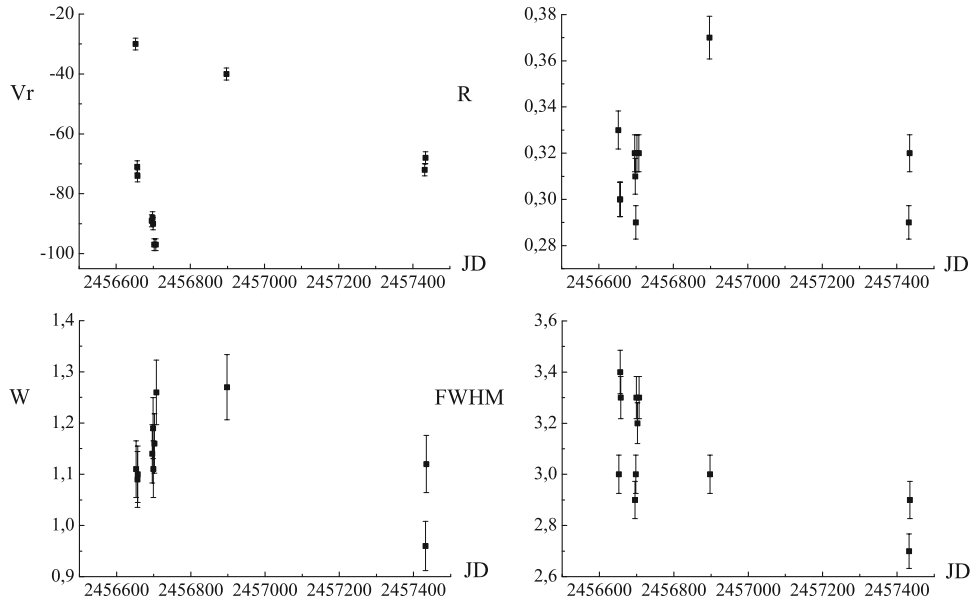

Figure 4. Variation with time of the radial velocities, equivalent widths, depths and half-widths in the Hβ. The error bars correspond to the measurements errors: radial velocity is $\sim \pm 2\,\mathrm{km\,s^{-1}}$, the depth and half-widths are ∼2.5% and equivalent width is ∼5%.

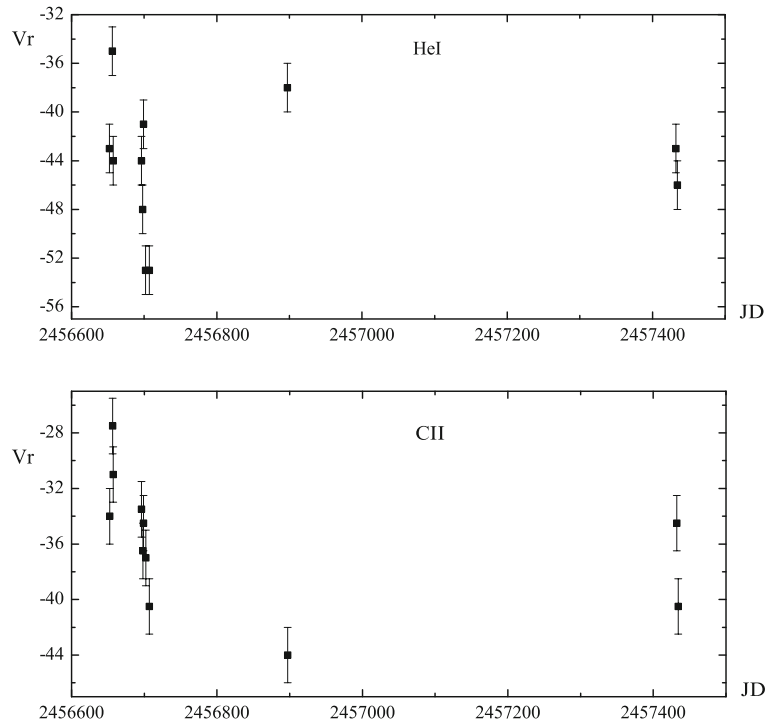

Figure 5. Variation with time of the radial velocities in the HeI λ5875.72 Å and averaged CII (λ6578.05 Å, λ6582.88 Å) lines in the spectra of HD14134 observed in 2013, 2014 and 2016. Error bars for the radial velocity is ∼± 2 km s $^{-1}$.

3.2 *Kinematic slice of the stellar atmosphere*

We estimated the radial velocities of the strong and basically weak absorption lines formed in deeper layers of the atmosphere (Klochkova & Chentsov 2004). All measurements were presented in Table 4.

Table 4 lists the heliocentric radial velocities of absorption lines of averaged two spectra taken on the

Table 4. The identification of lines, residual intensities (r) and heliocentric radial velocities (V_r) in spectra HD14134.

Lines	λ (Å)	r	V_r (km s^{-1})	Lines	λ (Å)	r	V_r (km s^{-1})
CII	6582.88	0.822	−35	NII	5495.67	0.979	−38
CII	6578.05	0.772	−39	SII	5473.62	0.960	−40
Hα	6562.82	0.881	−142	SII	5453.83	0.906	−40
NeI	6506.53	0.966	−43	SII	5432.82	0.942	−44
NII	6482.05	0.953	−38	SII	5428.67	0.968	−41
NeI	6402.25	0.936	−43	SII	5345.72	0.982	−41
NeI	6382.99	0.981	−44	SII	5320.73	0.966	−44
SiII	6371.36	0.898	−46	FeII	5316.65	0.993	−39
SiII	6347.10	0.861	−43	FeIII	5193.89	0.980	−40
NeI	6163.59	0.981	−43	FeII	5169.03	0.951	−43
NeI	6143.06	0.971	−42	OII	5160.02	0.991	−41
NeI	6074.34	0.984	−43	FeIII	5156.12	0.947	−38
HeI	5875.72	0.623	−53	CII	5145.16	0.977	−43
NaI D1	5889.95	0.264	−24	CII	5133.12	0.978	−43
NaI D2	5895.92	0.352	−21	HeI	5047.74	0.877	−44
FeIII	5833.93	0.972	−41	NII	5045.10	0.939	−43
NII	5747.30	0.984	−41	SII	5027.22	0.974	−46
SiIII	5739.73	0.910	−47	FeII	5018.44	0.971	−40
AlIII	5722.73	0.934	−46	HeI	5015.68	0.770	−46
NII	5710.77	0.956	−43	NII	5007.33	0.973	−40
AlIII	5696.60	0.898	−40	NII	5005.15	0.933	−41
NII	5686.21	0.955	−43	NII	5001.40	0.907	−43
NII	5679.56	0.867	−39	SII	4994.36	0.975	−40
NII	5676.02	0.940	−44	SII	4991.97	0.980	−43
NII	5666.63	0.924	−43	OII	4941.12	0.978	−40
SII	5659.99	0.972	−45	HeI	4921.93	0.715	−47
SII	5647.03	0.963	−42	SII	4917.21	0.972	−39
SII	5639.97	0.913	−40	Hβ	4861.34	0.681	−97
SII	5606.15	0.961	−42				

Here, all measurements are the average values of two spectra taken on the same night of February 13, 2014.

same night of February 13, 2014. The velocities are measured from the absorption cores of the entire profiles of their clearly identified components. We constructed the $V_r(r)$ curve for HD14134 (Fig. 6) and averaged the values of velocities of all photospheric absorption lines and determined for mean velocity, $V_r' = -42.2\,\mathrm{km\,s^{-1}}$. This value is the heliocentric velocity corresponding to the mass centre of the star. As seen it is close to the velocity $V_r = -43.4\,\mathrm{km\,s^{-1}}$ found by Gontcharov (2006) which is presented in Simbad Astronomical Database.

Such a plot (Fig. 6) shows the intervals of the depths of the lines found in the given spectrum and the velocities measured from these lines, and, it is immediately obvious from such a plot that the lines are associated with each other. If the dependence of V_r on r exists, it can be considered as a 'kinematic slice' of the atmosphere. In reality, we do not deal with a precise dependence of the expansion or contraction velocity of a certain atmospheric layer on its radius. We only mean the following: given that the residual intensity of absorption increases with optical depth, the shift toward smaller r in the plot, i.e., from left to right in Fig. 6, corresponds to ascension from lower to the upper atmospheric layers. It shows that the Hα absorption component shows the largest negative shift relative to weak lines. Such a shape of the $V_r(r)$ curve is characteristic of the majority of the B-supergiants (Chentsov *et al.* 2003).

The radial gradient of velocity in the atmosphere of a hot supergiant, which determines the magnitude of differential line shifts and which affects the shape of the $V_r(r)$ curve, increases both with temperature and luminosity.

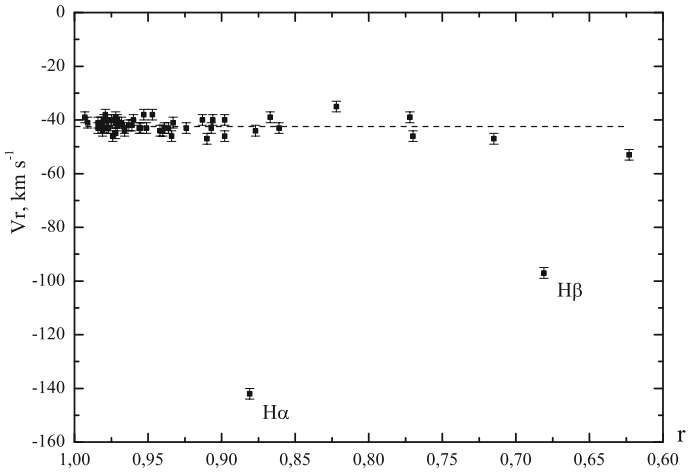

Figure 6. Relationship between the radial velocities (V_r) and residual intensities (r) of the absorption lines and absorption components of P-Cyg-type profiles in the spectra of HD 14134. The data plotted for all lines is the average values of two spectra taken on the same night of 13/02/2014. HeI, NeI, CII, NII, SII, OII, SiII, FeII, SiIII, FeIII and AlIII absorption lines were used for this. Here, filled circles represent the separate lines of components. The dashed line is the averaged velocity of the absorption lines. In addition, Balmer lines of hydrogen (Hα and Hβ) were presented too. Error bar for the radial velocity is $\sim\pm$ 2 km s $^{-1}$.

We note that even a small collection of $V_r(r)$ curves demonstrates their usefulness, at least for generalizing observational data on the kinematics of the atmospheres of supergiant stars and tracking its temporal variations. They are not as informative as the $V_r(\tau)$ dependences, but are also individual: each object has its individual curve with a characteristic albeit variable shape.

In addition, the sequences of the variations of the radial velocities of CII $\rightarrow$ HeI $\rightarrow$ Hβ $\rightarrow$ Hα lines has been considered in all phases which are formed in different depths of the atmosphere.

4. Discussion

The Hα profile of the hydrogen presented a complicated structure and a time variation for HD14134. The dramatic variations previously reported in HD14134 (Kudritzki *et al.* 1999; Morel *et al.* 2004) is also seen in our data.

In the Hα line profile, we detected the strong night-to-night intensity and profile shape variability. For 55 Cyg star, Kraus *et al.* (2015) concluded that it indicates rapid changes in the wind that might be interpreted as local material enhancements, caused by short-term mass ejection events traveling through the Hα line-forming region.

4.1 *Normal P-Cyg profile of Hα*

The profile of the Hα line which was observed on February 07, 09, 10, 13 and 18, 2014, are normal P-Cyg profiles with asymmetric absorption components. At these times the radial velocities of absorption and emission components of the Hα lines varied between -179 km s^{-1} to -88 km s^{-1} and $7-17$ km s^{-1}, respectively.

For example, we can see from Table 4 that on February 13, 2014 (Fig. 6), the radial velocities of lines Hα, Hβ and the average velocity of the HeI lines are -142 km s^{-1}, -97 km s^{-1} and -47.5 km s^{-1}, respectively. But the average velocities of the photospheric absorption lines are approximately same as the velocity of mass center. From this observational fact, we can also conclude the dynamical stability of the very deeper layers in which photospheric absorption lines are formed.

As seen, the radial velocities of only Hα and Hβ lines differ sharply from the velocity of the mass center of the star. If we take into account the velocity of mass center ($V_r' = -42.2$ km s^{-1}), we determine the values of -99.8 km s^{-1}, -54.8 km s^{-1} and -5.3 km s^{-1} for Hα, Hβ and the average velocity of the HeI lines, respectively. We can conclude that at that time there is an increasing rate of movement to the upper layers of the atmosphere i.e. there is an outflow of matter from the star. This observational fact suggests that at this phase the atmosphere of the star has an activity and it indicates that there is a matter flow to the upper layers of the stellar atmosphere and this star is surrounded by an envelope (Ebbets 1982).

On the other hand, when the normal P-Cyg profile of Hα is observed the sequences of differential shifts of CII $\rightarrow$ HeI $\rightarrow$ Hβ $\rightarrow$ Hα lines show that the velocity

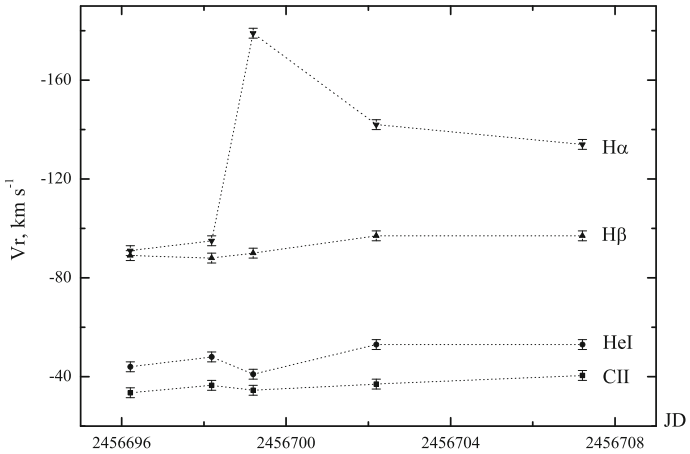

Figure 7. Variations of the radial velocities of CII, HeI, Hβ and Hα absorption lines when Hα line observed in the normal P-Cyg form. Error bar for the radial velocity is $\sim\pm 2$ km s $^{-1}$.

of expansion of lower layers is very slow than the upper layers (see Tables 2, 3 and Fig. 7).

So, in this case, the atmosphere of the star is in the expansion phase and is non-stationary.

4.2 *Inverse P-Cyg profile of Hα*

On December 25, 2013 and on August 27, 2014, we observed the inverse profile of line Hα. First, we determine the escape velocity from the star:

$$V_{\rm esc} = \sqrt{2G\frac{M_*}{R_*}} = \sqrt{2\times 6.67\times 10^{-11}\times\frac{24M_\odot}{52R_\odot}} \approx 420\,{\rm km\,s^{-1}}.$$

Here $M_\odot = 2\cdot 10^{30}$ kg and $R_\odot = 7\cdot 10^8$ m. Tables 2, 3 and 4 show that the observed velocities are much smaller than the escape velocity, and therefore, matter is not escaping from the star. That is, the material is driven away from a star's surface, but not maintained to escape speed, it can readily fall back directly onto the star. It indicates that formation of the inversion may be explained by the high-velocity motion of the stellar wind matter away from the observer. Wolf & Stahl (1990) and Wolf (1994) also explained this behaviour as the ejection of a large amount of gas making an expanding envelope, followed by a falling back of matter to its inner part.

We noted that when the inverse Hα profile is observed, the Hβ line is displaced to the longer wavelengths. As seen from Table 2, on these dates the absorption of Hα line shifted toward the red and, V_r(abs) $= -13$ km s^{-1} and V_r(abs) $= -31$ km s^{-1}, respectively. At the same time, Fig. 1(b) and Table 3 also show that, the Hβ line is also strongly redshifted and $V_r = -30$ km s^{-1} and $V_r = -40$ km s^{-1}, respectively. This suggests that such synchronous changes of Hβ line may be due to the result of a strong stellar wind away from the observer.

But Table 3 shows that the synchronous changes of the radial velocities of CII and HeI lines were not observed.

If we take into account the $V_r' = -42.2$ km s^{-1}, we see that in this case, the star atmosphere shows a contraction phase (especially for the upper layers) and is non-stationary.

4.3 *Disappearance of Hα profile*

Our observations showed that the intensity of the Hα line sharply weakened on February 13, 2016, and on the other hand the Hα line almost completely disappeared on December 29–30, 2013, and on February 15, 2016, in the spectra of the star HD14134 which probably is a manifestation of some recurrent processes in the star atmosphere.

Note that most authors (Rosendhal 1973; Kontizas & Kontizas 1981; Lennon *et al.* 1993; Kudritzki *et al.* 1999; Klochkova & Chentsov 2004; Morel *et al.* 2004; Crowther *et al.* 2006; Kraus & Fernandes 2009; Clark *et al.* 2010 and others) studied with spectroscopic investigation of this star. They remarked that in their spectra the Hα line maintained a P-Cyg profile, with highly variable strength. But we see that they did not mention the disappearance of Hα line in their studies. It shows that we have observed the disappearance of Hα line in the spectra of HD14134 for the first time.

We suggest that, when the matter of the stellar wind moves away from the observer, the absorption component of the Hα line is shifted toward the red region of the spectrum. Thus, the central frequencies (or wave lengths) of the absorption and emission components can coincide and compensate each other, which may lead to the disappearance of the Hα profile. That is, the disappearances of the Hα line may be related to 'swamping' of the absorption by emission.

Table 3 shows that at the time of the disappearance of the Hα line or when its intensity sharply weakens, the Hβ line is displaced to the relatively longer wavelengths and its radial velocities are $-71\,\mathrm{km\,s^{-1}}$, $-74\,\mathrm{km\,s^{-1}}$, $-72\,\mathrm{km\,s^{-1}}$ and $-68\,\mathrm{km\,s^{-1}}$, respectively. These observations may provide evidence for the fact that in the epochs when the Hα line becomes faint, the layer of matter where Hβ forms moves to the observer with lower velocity. However, the synchronous changes of the radial velocities of the other lines were not observed.

Hα and Hβ lines are known to form in the upper layers of the stellar atmosphere, in the region of generation of the stellar wind (Klochkova & Chentsov 2004; Zeinalov & Rzaev 1990). The variability of this region of the atmosphere implies the variability of those lines.

The observed complex wind structures seen in the Hα variability of the hot supergiants (Kaufer *et al.* 1996; Markova *et al.* 2008) imply that these objects cannot have smooth spherically symmetric winds.

These events may be a manifestation of a non-stationary atmosphere of the supergiant or a non-spherical stellar wind (Rosendhal 1973; Sobolev 1947, 1985; Pasok & Kolka 1992).

And which phase of the atmosphere is the disappearance of Hα?

Tables 2 and 3 show that the sequences of differential shifts of CII $\rightarrow$ HeI $\rightarrow$ Hβ $\rightarrow$ Hα lines in phases of disappearance of Hα are not similar to the ones in phases of inversion of Hα. So, if we take into account the velocity of mass center ($V_r' = -42.2\,\mathrm{km\,s^{-1}}$), then in phases of disappearance of Hα we observe that the deeper layers (CII, HeI, etc.) of the atmosphere is almost quiet, but the layers where Hβ forms is expanding. It is also shown in Table 3 that the velocity of the expansion of the layers where Hβ forms has slowed down at those times, that is, the Hβ lines is relatively redshifted. It can be explained that the flow of matter toward the star occurred and this event has influenced to the layers where Hβ formed. That is, in this case, the upper most layers of the star's atmosphere where Hα forms are in the contraction phase and are non-stationary. But the layers where Hβ forms are in the relative expansion phase, and the lower layers are in the quiet phase. Therefore we suggest that disappearance of Hα is, so to speak, the mixed conditions phase of the atmosphere.

We determined three different types of movement of matter: the expansion, the contraction and the mixed conditions. Note that the variations of the physical conditions (expansion, contraction and mixed phases) of the stellar atmosphere were explained in detail by Zeinalov & Rzaev (1990).

Hence, observations show that complete absence and inverse P-Cygni profile of Hα line are not accompanied by synchronous changes of the spectral parameters of the other lines formed in deeper layers of the stellar atmosphere (except Hβ), so it is most likely due to the physical processes occurring in the upper atmosphere.

Also, the relatively large changes in radial velocity of a sample of three absorption lines (CII λ 6578.05 Å, λ 6582.88 Å and HeI λ 5875.72 Å) of the other days were also observed. Pulsation instability as a possible cause of photospheric variability is suggested (Markova & Valchev 2000).

We noted above that the Hα line is formed in the upper most atmosphere of the star, i.e., in layers where the variable stellar wind is generated (Zeinalov & Rzaev 1990). Based on observations of different types of line profiles in the spectra of supergiant stars, it can be concluded that non-stationary processes reflected in the line profiles occur in their envelopes. It is known that variable wind and its accelerated motion in supergiants is caused by the strong flux of radiation from the star (De Jager 1984). Thus, the stellar radiation flux and the variable stellar wind lead to corresponding changes in the outer layers of the atmosphere and the star envelope (Kudritzki *et al.* 1999; Morel *et al.* 2004). As a result, we observe variable absorption and emission components of different forms of the Hα line P-Cyg profile of the star HD14134. Non-spherically, outflow of matter at different speeds and of different densities is observed for almost all supergiant stars (Sobolev 1947, 1985; Rosendhal 1973).

On the other hand, as is known, the variable stellar wind in the supergiants is caused by the pulsation (Cox 1983). If the dramatic changes of the Hα profile in the spectra of HD14134 is associated with the pulsation, they should occur periodically. But the amount of obtained data and their inconsistency in observation time does not make it possible to find such period in this study.

So, it is obvious that the Hα profile of HD14134 is strongly variable, exhibiting a large diversity of profile shapes and behaviour patterns. Similar patterns were observed in the spectra of HD225094 (Pasok &

Kolka 1992). According to Pasok & Kolka (1992), the mechanism that might be responsible for the observed variations is the growth of the envelope of the star with a following throw off of matter contained in it and/or 'puffs' lacking spherical symmetry.

We also suggest that the variations are explained probably by stellar wind properties (Kudritzki *et al.* 1999; Morel *et al.* 2004; Pasok & Kolka 1992) and/or pulsations mechanisms (Maeder 1980; Lovy *et al.* 1984).

5. Conclusions

It is the first time that the P-Cyg type profile of the Hα line has been found to occasionally disappear in the spectra of the supergiant star HD14134. It may be the result of the interaction of the variable stellar wind with the flux of material directed away from the observer. We suggest that the emission component is compensated by the shift toward the red side absorption component in the Hα profile and which may lead to the disappearance of this profile.

The mechanism that might be responsible for the observed variations is the growth of the envelope of the star with a following ejection of matter or non-spherical stellar wind (Pasok & Kolka 1992).

The inversion of the Hα profile is especially interesting. Formation of the inversion is explained as follows: the material is driven away from a star's surface, but not maintained to escape speed, it can readily fall back down directly onto the star.

Sometimes, the relatively large changes in radial velocity of the photospheric absorption (CII and HeI) lines is caused by the pulsation instability (Markova & Valchev 2000).

Hence, we found that the largest variations are displayed by the absorption and emission components of the Hα line, which indicates changes in the physical condition in the atmosphere and in the expanding stellar envelope. The repetition of the normal and inverse P-Cyg profiles, as well as the disappearance of the Hα line is mainly accompanied by expansion, contraction and mixed conditions of the star atmosphere, respectively.

Acknowledgements

The author is grateful to the reviewers for their attention to this study. This work was supported by the scientific program for the priority fields of research of the National Academy of Sciences of Azerbaijan.

References

Barlow, M. J., Cohen, D. 1977, Infrared photometry and mass loss rates for OBA supergiants and of stars, *Astrophys. J.*, **213**, 737.

Chentsov, E. L. *et al.* 2003, An atlas of spectra B6-A2 hypergiants and supergiants from 4800 to 6700 Å, *Astron. Astrophys.*, **397**, 1035.

Clark, J. S. *et al.* 2010, A serendipitous survey for variability amongst the massive stellar population of Westerlund 1, *Astron. Astrophys.*, **514** A87, 1.

Cox, J. P. 1983, *Theory of Stellar Pulsation*, Mir, Moscow.

Crowther, P. A., Lennon, D. J., Walborn N. R. 2006, Physical parameters and wind properties of galactic early B supergiants, *Astron. Astrophys.*, **446**, 279.

De Jager. C. 1984, *The Brightest Stars*, Mir, Moscow.

Ebbets, D. 1982, The structure and variability of Hα emission in early-type supergiants. *Astrophys. J. Suppl. Ser.*, **48**, 399.

Galazutdinov, G. A. 1992, "Stellar Echelle Spectrum Processing System", Preprint SAO RAN, Spets. Astrofiz. Nizhnii Arkhyz, KChR, 92.

Gontcharov G. A. 2006, Pulkovo compilation of radial velocities for 35495 Hipparcos stars in a common system, *Astron. Lett.*, **32(11)**, 759.

Kaufer, A. *et al.* 1996, Long-term spectroscopic monitoring of BA-type supergiants, I. Hα line-profile variability, *Astron. Astrophys.*, **305**, 887.

Klochkova V. G., Chentsov E. L. 2004, The optical spectrum of an LBV candidate in the Cyg OB2 association, *Astron. Rep.*, **48**, 1005.

Klochkova V. G. *et al.* 2014, Spectral variability of the IR source IRAS01005+7910 optical component, *Astrophys. Bull.*, **69**(4), 439.

Kontizas E., Kontizas M. 1981, Radial velocities for different spectral lines of B and A supergiants in our Galaxy and in the large magellanic cloud, *Astron. Astrophys. Suppl. Ser.* **45**, 121.

Kraus, M., Fernandes, M. B. 2009, Parameters of galactic early B supergiants; the influence of the wind on the interstellar extinction determination, *Astron. Astrophys.*, **499**, 291.

Kraus, M. *et al.* 2015, Interplay between pulsations and mass loss in the blue supergiant 55 Cygnus = HD198478, *Astron. Astrophys.*, **581**, A75, 1.

Kudritzki, R. P. *et al.* 1999, The wind momentum-luminosity relationship of galactic A and B supergiants, *Astron. Astrophys.*, **350**, 970.

Lennon, D. J. *et al.* 1993, Galactic B-supergiants; line strengths in the visible-evidence for evolutionary effects, *Astron. Astrophys. Suppl. Ser.*, **97**, 559.

Lovy, D. *et al.* 1984, Supergiant variability: theoretical pulsation periods and comparison with observations, *Astron. Astrophys.*, **133**, 307.

Maeder, A. 1980, Supergiant variability: amplitudes and pulsation constants in relation with mass loss and convection, *Astron. Astrophys.*, **90**, 311.

Markova N., Valchev, T. 2000, Spectral variability of luminous early type stars. I. Peculiar supergiant HD199478, *Astron. Astrophys.*, **363**, 995.

Markova N. *et al.* 2008, Wind structure of late B supergiants, I. Multi-line analyses of near-surface and wind structure in HD199478 (B8Iae), *Astron. Astrophys.*, **487**, 211.

Mikailov, Kh. M., Khalilov, V. M., Alekberov I. A. 2005, Cassegrain echelle spectrometer of the 2-m telescope of ShAO NAS Azerbaijan, *Tsirk. Shamakhy Astrophys. Observ.*, **109**, 21.

Morel, T. *et al.* 2004, Large-scale wind structures in OB supergiants: a search for rotationally modulated Hα variability, *Mon. Not. R. Astron. Soc.*, **351**, 552.

Morton, D. C. 1967, Mass loss from three OB Supergiants in Orion, *Astrophys. J.*, **150**, 535.

Pasok, A., Kolka, I. 1992, The Hα profile variations in the spectrum of HD225094, B3Ia, IBVS, 3804.

Prinja R. K. *et al.* 1996, Variability in the optical wind lines of HD151804 (O9Iaf), *Astron. Astrophys.*, **311**, 264.

Rosendhal, J. D. 1973, A survey of Hα emission in early-type high-luminosity stars, *Astrophys. J.*, **186**, 909.

Santolaya-Rey, A. E., Puls, J., Herrero A. 1997, Atmospheric NLTE-models for the spectroscopic analysis of luminous blue stars with winds, *Astron. Astrophys.*, **323**, 488.

Sobolev, V. V. 1947, "Moving Envelopes of Stars", Leningrad

Sobolev, V. V. 1985, "Course in Theoretical Astrophysics" Izdatel'stvo Nauka, Moscow.

Stahl, O. Wolf B. 1986, Circumstellar shells around luminous emission-line stars in the Large Magellanic Cloud, *Astron. Astrophys.*, **158**, 371.

Swings, P., Struve, O. 1940, Spectrographic Observations of Peculiar Stars, *Astrophys. J.*, **91**, 546.

Vardya, M. S. 1984, Dimensional approach to mass loss: O- and B-type stars, *Astrophys. Space Sci.*, **107**, 141.

Wolf, B. 1994, Investigation of LBV of the Magellanic Clouds during the past decade with LTPV, Caspel and IUE, in: C. Sterken & M. de Groot (eds), *The impact of long-term monitoring on variable star research*, vol. 191 (Drodrecht: Kluwer Acad. Pub.).

Wolf B., Stahl, O. 1990, Inverse P Cygni-type profiles in the spectrum of the Luminous Blue Variable S Doradus, *Astron. Astrophys.*, **235**, 340.

Zeinalov, S. K., Rzaev, A. Kh. 1990, Non-stationary atmospheres of supergiants, *Astrophys. Space Sci.*, **172**, 211.